Journal of Hydrology 522 (2015) 239–249

Contents lists available at ScienceDirect

Journal of Hydrology

journal homepage: www.elsevier.com/locate/jhydrol

# Evaporative fractions and elevation effects on stable isotopes of high elevation lakes and streams in arid western Himalaya

Trent W. Biggs [a,*], Chun-Ta Lai [b], Pankaj Chandan [c], Raymond Mark Lee [a], Alex Messina [a], Rebecca S. Lesher [a,d], Nisa Khatoon [c]

[a] Department of Geography, San Diego State University, 5500 Campanile Drive, San Diego, California, 92182, United States
[b] Department of Biology, San Diego State University, 5500 Campanile Drive, San Diego, California, 92182, United States
[c] High Altitude Wetlands Conservation Programme, Worldwide Fund for Nature – India, Delhi, India
[d] Oneida Total Integrated Enterprises, Inc., Honolulu, Hawaii, United States

ARTICLE INFO

*Article history:*
Received 15 May 2013
Received in revised form 23 October 2014
Accepted 13 December 2014
Available online 22 December 2014
This manuscript was handled by Laurent Charlet, Editor-in-Chief, with the assistance of Pedro J. Depetris, Associate Editor

*Keywords:*
Water balance
Closed basin
Mountain hydrology

SUMMARY

Isotopes of oxygen and hydrogen in water from streams, snow, and lakes were used to model the ratio of evaporation to total inflow ($E/I$) of four high elevation lakes in closed basins in the Indian Himalaya. Air temperature and relative humidity ($h$) data from meteorological stations and global climate grids (GMAO-MERRA) were used as input to the model. A second model of the volume of inflow during snowmelt constrained the magnitude of seasonal variability in isotopic composition. Similar to other areas of the Himalaya, elevation was a strong determinant of isotopic composition of stream water, suggesting that heavier isotopes rain out at lower elevations. Deuterium excess ($d$) in stream water suggests that summer precipitation originating from the Bay of Bengal rather than winter precipitation from Central Asia is the dominant source of precipitation. For the largest and deepest lakes (>15 m), $E/I$ was 77–87%, and 18–50% for two shallow lakes (<2 m). Modelled $E/I$ was sensitive to $h$; ground-level measurements of h are needed to constrain $E/I$ estimates in arid mountain regions, though $h$ from GMAO also produced reasonable $E/I$ values. The results suggest that some lakes in closed basins in the Himalaya lose a significant fraction of their inflow to groundwater, particularly shallow lakes with a low ratio of lake volume to watershed area. Isotopic values from the mainstem of the Indus River suggest that evaporatively enriched waters have limited impact on both wet and dry season discharge at the basin scale. Lakes with a high evaporative fraction may be uniquely sensitive to climate, and isotopic analysis can help identify lakes that may be vulnerable to climate fluctuations and change.



## 1. Introduction

Lakes play important roles in the hydrology and ecology of mountainous regions. Lakes can either increase dry season streamflow by recharging local or regional groundwater, or decrease dry season streamflow by increasing evaporation (Bullock and Acreman, 2003). Significant uncertainty remains about the influence of high elevation lakes on monthly and annual streamflow. The hydrology of lakes in closed basins, which have no surface outlet, can be particularly difficult to determine since the main outflow is through recharge to groundwater. Lakes in closed basins may impact regional hydrology through subsurface flow, which is difficult to quantify, and is usually calculated as a residual in the water balance. Given the likelihood of significant changes in the hydrology of the Himalaya due to climate change (Immerzeel et al., 2010), it is imperative to understand the role that high elevation lakes play in the seasonal and annual water balance of Himalayan river systems. There is currently very little information on the role of evaporation and subsurface flow in the annual hydrologic budget of Himalayan lakes in closed basins. An interannual water balance on one of the largest lakes in the Tibetan Plateau (Nam Co) suggests that more than half of the inflow to the lake is lost through groundwater seepage, with important implications for the water balance of the Tibetan Plateau and receiving water bodies (Zhou et al., 2013).

Evaporation as a fraction of inflow to a lake ($E/I$) can be calculated using oxygen ($^{18}O$) and deuterium (D) isotopes and a model of isotopic fractionation during evaporation (Dincer, 1968; Gibson and Edwards, 2002; Krabbenhoft et al., 1990; Zuber, 1983). $E/I$ models are based on the evaporative enrichment of $^{18}O$ and D, which evaporate at lower rates than $^{16}O$ and $^{1}H$. The

* Corresponding author. Tel.: +1 619 594 0902; fax: +1 619 594 4938.
*E-mail address:* tbiggs@mail.sdsu.edu (T.W. Biggs).

http://dx.doi.org/10.1016/j.jhydrol.2014.12.023
0022-1694/

departure of $\delta^{18}O$ and $\delta D$ in a sample from the global meteoric water line (GMWL) is proportional to $E/I$. Isotopic techniques are particularly useful where there are no discharge measurements to constrain a water balance, as is the case for many remote regions. Applications of $E/I$ models include regional sampling in the Canadian Arctic (Gibson and Edwards, 2002; Gibson et al., 2002), where $E/I$ decreased with increasing latitude. While regional surveys of the isotopic composition of water have been conducted in the Himalaya (Bartarya et al., 1995; Pande et al., 2000), and isotopes have been used to quantify surface–groundwater exchange in lakes at the foothills of the Himalaya (Nachiappan and Kumar, 2002), the meteorological data required to perform an isotopic water balance have not typically been available, nor have isotopic measurements been used to estimate $E/I$ for lakes in the Himalaya.

Both stable isotopes of water ($^{18}O$ and D) can be used to estimate $E/I$ and to test the validity of model assumptions. Zuber (1983) applied the $E/I$ model to several lakes that had complementary water balance data, and documented that the field-observed kinetic enrichment of D during evaporation is sensitive to humidity ($h$), showing significant departures from values determined in laboratory experiments under conditions of moderate to low $h$ (<70%). This is potentially important for modelling the water balance using isotopic methods in semi-arid and arid regions.

The meteorological data required to implement isotopic $E/I$ models include air temperature and $h$, which may not be readily available in remote regions. Global gridded data, like that from the Global Meteorological Analysis Office (GMAO) could be used as input, though their cell sizes (e.g. 0.67°) may complicate their use in mountainous environments. $E/I$ values may also be impacted by seasonal inflow of isotopically light water that has not been impacted by evaporation, including snowmelt (Gibson et al., 2002). Implementation of $E/I$ models requires an estimate of uncertainty and evaluation of model sensitivity to meteorological inputs and model assumptions.

Isotopes of water have also been used to reconstruct paleoelevations of mountain ranges based on the relationship between elevation and isotope composition in modern and paleowater samples (Garzione et al., 2000). Regional variations in the elevation–isotope relationship complicate such reconstructions (Hren et al., 2009), and the elevation–isotope relationship may weaken at high elevations (Pande et al., 2000), so additional documentation of the elevation–isotope relationship in sparsely-sampled environments is required, particularly at high elevations in remote regions of the Himalaya. Data on $^{18}O$ and D, in particular the deuterium excess ($d$) can also help identify the dominant sources of moisture in precipitation, streams and groundwater (Weyhenmeyer et al., 2002). In the Himalaya, they have been used to quantify the relative contribution of moisture from the Bay of Bengal to the east during the Indian Summer Monsoon and from central Asia to the west and north during the winter (Hren et al., 2009; Karim and Veizer, 2002; Maurya et al., 2011).

The objective of this study is to use a combination of water balance modelling, meteorological measurements and isotopic analyses of stream water, lake water and snow to estimate the roles of evaporation and subsurface discharge in the annual water balance of four high elevation lakes located in closed basins in the Indian Himalaya. A secondary objective is to document the regional elevation–slope relationship and deuterium-excess and compare them with other regional studies. The main research questions are: What fraction of the inflow to high elevation lakes is evaporated, estimated using an $E/I$ model and data on $^{18}O$ and D? How sensitive are $E/I$ estimates to input meteorological data and potential seasonal variations in isotopic composition? Are differences in the evaporative fractions related to lake depth or watershed characteristics? How does stream water isotopic composition change with elevation? What do deuterium excess values in streamflow suggest about the dominant sources of moisture for precipitation?

## 2. Study area

The study area includes four lakes in the Ladakh region of the Indian Himalaya in the State of Jammu and Kashmir, south and east of the city of Leh (Fig. 1, Table 1). Two lakes are relatively deep, and two are shallow (Table 1). The first and largest lake, Tso Moriri, lies at an elevation of 4535 m.a.s.l. Its watershed is part of the Sutlej sub-basin of the Indus River. Based on Landsat TM imagery from 1972–2009, the surface area of Tso Moriri ranges from 139.7 to 145.1 $km^2$ (Lesher, 2011) compared to 148.8 $km^2$ recorded by Hutchinson (1937). The mean and maximum depths are 55 m and 75.5 m (Hutchinson, 1937). Two main tributaries enter the lake, one each at the northern and southern ends (Fig. 1). Visual interpretation of daily satellite imagery from the Moderate Resolution Imaging Spectroradiometer (MODIS) between 2001 and 2010 suggest that Tso Moriri is frozen between 77 and 138 days of the year, with ice-on between 4 January and 16 February and ice-off between 29 April and 31 May (Lesher, 2011). The lake and nearby wetlands provide habitat for several important bird species, including the black-necked crane (Mishra and Humbert-Droz, 1998).

The second deep study lake, Kyagar Tso (elevation 4736 m), receives inflow from a watershed area of 64 $km^2$, and has a maximum depth of 21.2 m (Hutchinson, 1937). Topographically, it lies in the Tso Moriri watershed, but there is no visible evidence of surface water linkage between the two lakes, so the Kyagar Tso watershed is considered hydrologically closed (Hutchinson, 1937). The two shallow lakes (Tso Kar and Startsapuk Tso) are 40 km northwest of Tso Moriri in the Zaskar sub-basin of the Indus River. The smaller lake, Startsapuk Tso, has lower salinity and a surface outlet to the larger Tso Kar. The most commonly observed depths are approximately 1 m (Startsapuk Tso) and 2 m (Tso Kar) (Table 1). The two shallow lakes have a combined watershed area of 630 $km^2$.

The four lakes differ in the ratio of lake volume to watershed area (Table 1). The deeper lakes have a large volume:area ratio, indicating that they may be less sensitive to interannual variability in watershed inputs and likely have longer residence times than the two shallow lakes.

The region has very low annual precipitation. Records from the Indian Meteorological Department at Leh indicate that mean annual precipitation was 92 mm/year from 1973 to 1994 and 270 mm/year from 2002 to 2006. Between 1973 and 1994, 35% of the precipitation at Leh fell between June and September and 52% fell between December and March. Data from 2002 to 2006 suggest that most precipitation that falls between November and March or April is snow, so snow represented approximately 50% of total precipitation from 1973 to 1994. From 2002 to 2006, winter precipitation (December–March) represented a higher percentage of total annual precipitation (70%) compared to 1973–1994.

The lakes lie south of the Indus-Tsangpo Suture Zone in the Zanskar mountain range in the western section of the Himalayan-Tibetean orogen. The geology underlying the lakes includes sedimentary and metamorphic rock overlain by Quaternary sediments (Bagati and Thakur, 1993; Hedrick et al., 2011). The three smallest lakes lie entirely on the Tso Moriri nappe, which consists of Ordovician granite-gneiss and Precambrian to Cambrian metasediments (Schlup et al., 2003). Tso Kar is bounded on its northwestern end by Precambrian and Cambrian metasediments. Tso Kar and Startsapuk Tso are underlain by Quaternary fluvial and lacustrine deposits ranging from sandy gravel to clay (Bhattacharyya, 1989). Tso Moriri lies on the Tso Moriri nappe in

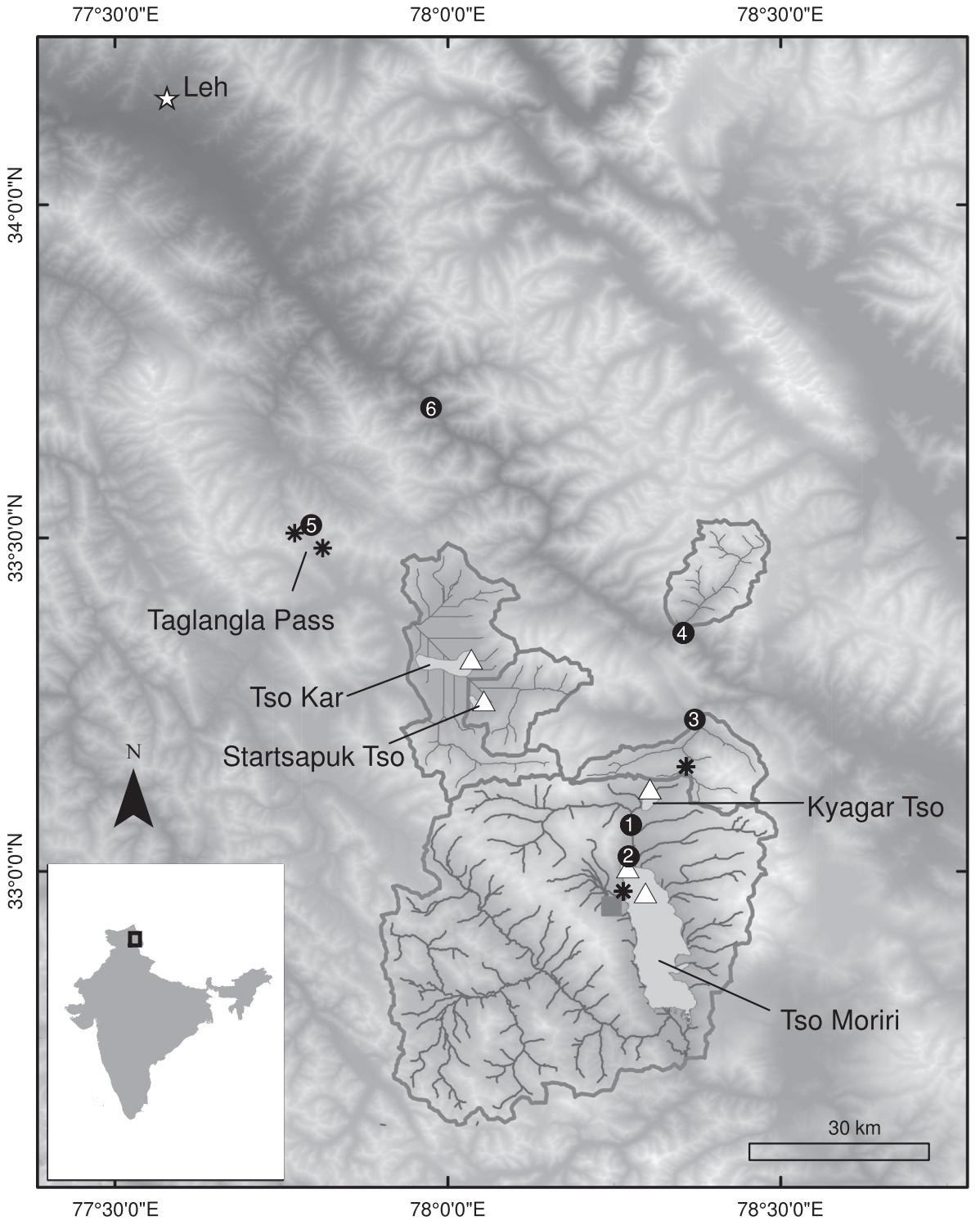


**Fig. 1.** Location map showing water sampling sites, including lakes (white triangles), streams (numbered black circles), and snow (asterisks). Meteorological data were from a site at Tso Moriri (grey square) and the city of Leh (white star). The numbers on the stream sampling sites correspond with the sample numbers in Table 3.

its northern section, and on the granite-gneiss of the Mata nappe in the south (Schlup et al., 2003). Tso Moriri is bounded on its southern end by Quaternary sediments that form an alluvial fan, which blocks the Tso Moriri river and formed the lake (Bagati and Thakur, 1993), consistent with the formation of other lakes in the region by the landslides and rapid erosion rates that occurred during intensified monsoon phases in the late Pleistocene and Holocene (Bookhagen et al., 2005).

Paleoclimate records derived from lake sediments at Tso Moriri and Tso Kar indicate that the climate is currently in a dry phase after a period of maximum precipitation between 11,000 and 9600 years before present (Leipe et al., 2014). Water levels in Tso Kar appear to be falling (Phartiyal et al., 2005) and lacustrine deposits on the shorelines of the other lakes indicate that water levels were higher in the early and mid-Holocene compared to the 20th century (Hutchinson, 1937). Tso Kar alternated between

**Table 1**
Characteristics of the four study lakes and the watersheds that drain to them. Lake surface area was taken from Hutchinson (1937) and from manual digitizing of high resolution imagery from Sept 1, 2013 (Google Earth). Mean depth is from Hutchinson (1937).

| | Tso Moriri | Kyagar Tso | Tso Kar | Startsapuk Tso |
|---|---|---|---|---|
| *Surface area ($A_L$), km²* | | | | |
| Hutchinson | 149 | 6.2 | 15.6 | 2.5 |
| Sept 1, 2013 | 145 | 5.0 | 19.7 | 3.7 |
| Mean depth ($D$), m | 55 | 15[a] | 2[b] | 1[b] |
| *Lake volume ($V_L = A_L D$) Mm³* | | | | |
| Hutchinson | 8195 | 91 | 31 | 3 |
| Sept 1, 2013 | 7975 | 75 | 39 | 4 |
| *Watershed area ($A_w$) (km²)* | 2361 | 64 | 458 | 172 |
| $V_L$:$A_w$ (m) | 3.5 | 1.4 | 0.07 | 0.02 |

[a] Depth at the centre.
[b] Approximate; most commonly observed depth.

brackish and fresh water during the Pleistocene and Holocene, indicating a variable climate (Bhattacharyya, 1989).

## 3. Methods

### 3.1. Isotope evaporation model

Stable isotopes of oxygen ($^{18}O$) and hydrogen (D) were used to constrain the water balance of the four studied lakes. The methods follow a combination of Gibson and Edwards (2002) and Gibson et al. (2002), which are based on isotopic mass balance. The main objective is to determine the fraction of inflowing water ($I$) that is evaporated from the lake surface ($E/I$), as:

$$\frac{E}{I} = \frac{\delta_L - \delta_I}{m(\delta^* - \delta_L)} \quad (1)$$

where $\delta_L$ is the measured isotopic composition of the lake, $\delta_I$ is the measured isotopic composition of inflow to the lake, including both precipitation on the lake surface and streamflow, $\delta^*$ is the isotopic composition of a lake evaporating to dryness in the given climate, and $m$ is the enrichment slope, which is a function of humidity and the total ($\varepsilon$) and kinetic ($\varepsilon_K$) isotopic separation factors, which are in turn functions of temperature. The calculation of $\varepsilon_K$ assumes turbulent transport from the lake surface to the atmosphere, which is a common approximation for natural lakes.

The enrichment slope ($m$) is calculated as:

$$m = \frac{h - 0.001\varepsilon}{1 - h + 0.001\varepsilon_K} \quad (2)$$

where $h$ is relative humidity (0–1) at the evaporating surface, and ε is the sum of the equilibrium separation factor ($\varepsilon_*$) and $\varepsilon_K$. $\varepsilon_*$ is calculated from mean monthly air temperature and $\varepsilon_K$ is calculated as $C_K(1 - h)$, where $C_K$ is experimentally determined as 14.2‰ for $\delta^{18}O$ and 12.5‰ for D (Gonfiantini, 1986). Zuber (1983) documented $\varepsilon_K$ values in field surveys of lake water balances, and found higher $\varepsilon_K$ values for D compared to that determined by laboratory experiments. The discrepancy becomes pronounced particularly for moderate to low humidity ($h < 0.7$). In this study, we used the $\varepsilon_K - h$ relationship described by Zuber (1983) when using D in the estimate of $E/I$.

The isotopic composition of the lake evaporating to dryness ($\delta^*$) is calculated as:

$$\delta^* = \frac{h\delta_A + \varepsilon}{h - 0.001\varepsilon} \quad (3)$$

where $\delta_A$ is the isotopic composition of atmospheric water vapour just above the evaporating surface, approximated by $\delta_A = \delta_P - \varepsilon_*$, where $\delta_P$ is the mean isotopic composition of precipitation, often assumed equal to $\delta_I$.

The saturation vapour pressure for calculating $h$ is usually taken as the air temperature at the water surface, though regional applications use interpolated values from meteorological stations given the difficulty of obtaining long time series of temperature and h at the lake surface (Gibson and Edwards, 2002). See Gibson and Edwards (2002) and Gibson et al. (2002) for additional details of the model.

In ice-covered lakes, the annual averages of $\delta^*$ and $m$ need to be flux-weighted by the fraction of total annual evaporation that occurs in a given month (Gibson et al., 2002). For all lakes except Tso Moriri, we assumed that evaporation rates corresponded to potential evaporation calculated using the Abtew method (Xu and Singh, 2000), which uses incoming shortwave radiation at the ground surface ($R_s$) and was recommended for use at another high-elevation lake (Titicaca) (Delclaux et al., 2007). $R_s$ was calculated as the product of incoming shortwave radiation at the top of the atmosphere and the atmospheric transmissivity ($\tau$). $\tau$ was calculated using an empirical equation that uses monthly precipitation as the predictor and was calibrated for the Tibetan Plateau (Matsuda et al., 2006). $\tau$ did not vary significantly by month, so we used the mean annual value (0.7). Evaporation was assumed zero for months with mean temperature less than 0 °C. The Hargreaves (Xu and Singh, 2000) and Thornthwaite (Dunne and Leopold, 1978) models were also used to estimate the monthly evaporation weights, but the equation used had very little impact on the modelled $E/I$, so the results from the Abtew model are presented here based on its performance at another high elevation lake (Delclaux et al., 2007). A 2-D model (CE-QUAL-W2) of the deepest lake (Tso Moriri) (Lesher, 2011) suggested there is a temporal lag between potential evaporation from the Abtew model and evaporation from the lake surface; evaporation was low or zero during the months the lake was frozen (January–May), even when mean daily $T_a$ was greater than zero (March–May), and evaporation reached a maximum in September through November after the lake water had warmed, and remained positive even for months with mean $T_a$ below zero. Due to these observed lags, the monthly evaporation weighting factor for Tso Moriri was calculated from the evaporation time series from the CE-QUAL-W2 model (Lesher, 2011).

The main assumptions of the isotopic $E/I$ model are that (1) the lake is at steady-state, so volume and isotopic composition are not changing appreciably with time. A time series of Landsat TM images shows that the lake area of Tso Moriri changed very little (<3%) from 1979 to 2009, with no monotonic change (Lesher, 2011), supporting the steady-state assumption on interannual time scales. Inflow of isotopically light water that has not undergone evaporative fractionation can also shift the isotopic composition of lake water towards the meteoric water line, with subsequent evaporative fractionation increasing the isotopic values during the rest of the year. The potential for seasonal changes in the isotopic composition of the lakes associated with snowmelt is explored in Section 3.4 using a snowmelt model. (2) The isotopic composition of precipitation on the lake surface is assumed equal to the isotopic composition of the inflow. The validity of this assumption has been well documented for several regions, including a site on the Tibetan Plateau (Tian, 2003), though it might be violated where the mean elevation of the watershed is significantly different from the elevation of the lake. (3) Atmospheric moisture is in isotopic equilibrium with precipitation. Assumptions 2 and 3 cannot be evaluated with the current data set. Assumption 1 is evaluated by determining the sensitivity of $E/I$ values to inflow from snowmelt in Section 3.4.

### 3.2. Data and sample collection

#### 3.2.1. Water samples

Stream water was sampled at six different locations, snow at six different locations, and lake water at four different lakes between May 29 and June 5, 2011 (Fig. 1). Snow was sampled at two locations near Tso Moriri immediately following a storm on June 2, 2011, and at four locations from pre-existing snowpack (Fig. 1). Stream water samples were grab samples taken from the channel thalweg. Lake water from Tso Moriri was sampled at 30 cm depth from a raft at two locations, one near the centre of the lake, and a second in the northern branch closer to the shore. Grab samples from Kyagar Tso, Tso Kar, and Startsapuk Tso were taken from the shoreline at approximately 30 cm depth. Snow samples were collected in clean plastic bottles, melted at room temperature and immediately transferred to a sample bottle. All sample bottles were filled to the top with no air space to prevent evaporation.

While samples from different depths are desirable for isotopic analysis of a lake, water temperature profiles at Tso Moriri suggested that it was not stratified at the time of sampling (5.7 °C at 0.2 m and 4.6 °C at 15 m, Appendix Fig. 1). Due to the cold water temperatures, evaporation from the surface and evaporative fractionation of the isotopic composition at the surface is also at a minimum immediately following ice melt (Table 2), suggesting that the lake was well-mixed with minimal evaporation since ice-off. Stratification was found to have a very small impact on isotopic water balance calculations in other cold regions (Gibson et al., 2002). Samples from lake shores may be evaporatively enriched if vegetation prevents mixing of water with the main lake water body or if there is bank storage of evaporatively enriched water that also does not mix with the main lake body (Gibson et al., 2002). There was minimal vegetation at all sampling sites and we assumed the lakes were well-mixed. In support of this assumption, water samples from the middle and near the shore of Tso Moriri (Fig. 1) showed nearly identical $\delta^{18}O$ values (see Results Section 4.2).

Time series of snow covered area ($A_{sc}$) in each watershed draining to the lakes were derived from the Moderate Resolution Imaging Spectroradiometer (MODIS) MOD10A2 product from January 1 to December 31, 2011. Water sampling occurred a week after a rapid decline in $A_{sc}$ (Fig. 2). At the northern tributary of Tso Moriri, water depth was 23 cm, which was 26% of the estimated bankfull depth (88 cm) and suggested that the stream was sampled under baseflow conditions.

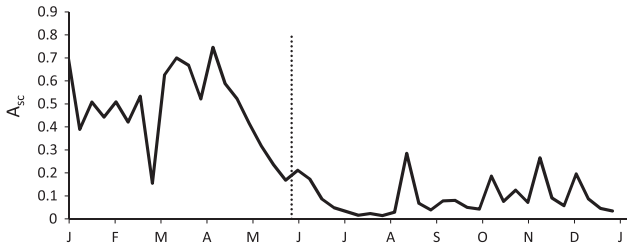


**Fig. 2.** Time series of snow covered area ($A_{sc}$) in the Tso Moriri watershed as a fraction of the watershed area in 2011. $A_{sc}$ was calculated from the MOD10A2 8-day snow covered area product. The vertical dashed line indicates the start of sampling (May 29, 2011).

#### 3.2.2. Meteorological data

The long-term mean monthly $T_a$ and relative humidity ($h$) at Tso Moriri and Tso Kar were determined using a combination of historical data at the Leh meteorological station (2000–2006, elevation 3514 m), meteorological field measurements from June 2011 to December 2011, and global climate grids. At Tso Moriri, $T_a$ and atmospheric pressure were recorded at 30 min intervals with a BaroTROLL™ from June 2, 2012 to December 14, 2012. An automated meteorological station at Tso Moriri measured rainfall, $T_a$ and $h$ at 30 min intervals from June 30, 2012 to August 21, 2012. The meteorological station and temperature loggers were installed on a short (~3 m) one story structure approximately 0.9 km from the lake shore.

An environmental lapse rate for temperature (LR) was calculated for each month using two data sources. First, LR was calculated from the BaroTROLL™ temperature logger installed at Tso Moriri and a temperature logger (TidBiT v2) installed in Leh (Grand Willow Hotel, hereafter GW), both of which measured $T_a$ at 30 min intervals from June 4, 2011 to December 14, 2011. LR was then applied to the average $T_a$ at Leh from 2000–2006 to give the long-term average monthly $T_a$ at each lake. $T_a$ data were not available at Tso Moriri from January to May so LR could not be calculated for those months, so we used the observed LR from June to December to estimate LR from January to May, assuming that mea-

**Table 2**
Meteorological data used for the evaporative fraction model. Mean monthly air temperature ($T_{av}$) at Leh, Grand Willow Hotel (LGW, 3466 m), Leh Meteorological Station (LMS, 2000–2006), and Tso Moriri (TM, 4574 m); lapse rates (LR) between LGW and TM based on the temperature loggers (Logr) and MODIS (MOD); relative humidity ($h$) at LMS from 2000–2006, at Tso Moriri in 2011, corrected $h$ at Tso Moriri (TM corr.), and from GMAO-MERRA grids at Leh (GMAO LMS) and Tso Moriri (GMAO TM). Evaporation weights (EW) are from a model of Tso Moriri (CEQ, Lesher, 2011) or Abtew method (Xu and Singh, 2000). EW were used to calculate flux-weighted average values of $\delta^*$ and $m$.

| | $T_{av}$ °C | | | LR[b] °C km$^{-1}$ | | $h$ (0–1) | | | | | | Precip mm | EW (0–1) | |
|---|---|---|---|---|---|---|---|---|---|---|---|---|---|---|
| | LGW | LMS | TM | Logr | MOD | LMS | TM obs. | TM corr. | GMAO LMS | | GMAO TM | LMS | CEQ | Abtew |
| | 2011 | 2000–2006 | 2011 | | | 2000–2006 | 2011 | | 2000–2006 | 1979–2012 | 1979–2012 | 1973–1994 | | |
| J | – | −6.2 | – | 4.5 | 4.4 | 0.67 | – | 0.60 | 0.46 | 0.49 | 0.51 | 14.2 | 0.01 | 0.00 |
| F | – | −3.0 | – | 6.3 | 6.2 | 0.64 | – | 0.57 | 0.50 | 0.50 | 0.52 | 10.5 | 0.00 | 0.00 |
| M | – | 2.8 | – | 6.8 | 7.4 | 0.58 | | 0.51 | 0.43 | 0.46 | 0.52 | 13.8 | 0.01 | 0.00 |
| A | – | 7.6 | – | 7.4 | 8.0 | 0.51 | – | 0.44 | 0.42 | 0.43 | 0.42 | 3.2 | 0.05 | 0.14 |
| M | – | 12.5 | – | 8.2 | 7.7 | 0.52 | – | 0.45 | 0.38 | 0.41 | 0.37 | 3.3 | 0.05 | 0.16 |
| J | 21.7 | 16.2 | 9.9 | 10.7 | 6.8 | 0.51 | – | 0.44 | 0.35 | 0.37 | 0.33 | 1.8 | 0.06 | 0.16 |
| J | 22.7 | 20.8 | 13.7 | 8.2 | 6.0 | 0.48 | 0.40 | 0.41 | 0.36 | 0.37 | 0.38 | 11.2 | 0.08 | 0.16 |
| A | 21.0 | 19.5 | 12.8 | 7.4 | 5.8 | 0.56 | 0.50 | 0.49 | 0.40 | 0.40 | 0.43 | 12.1 | 0.11 | 0.15 |
| S | 17.4 | 15.3 | 9.8 | 6.8 | 6.0 | 0.52 | – | 0.45 | 0.34 | 0.38 | 0.41 | 6.8 | 0.16 | 0.13 |
| O | 8.9 | 6.7 | 1.9 | 6.3 | 5.9 | 0.52 | – | 0.45 | 0.30 | 0.34 | 0.35 | 1.7 | 0.17 | 0.10 |
| N | 2.9 | 0.4 | −2.0 | 4.5 | 4.9 | 0.56 | – | 0.49 | 0.33 | 0.36 | 0.40 | 3.9 | 0.18 | 0.00 |
| D | −0.9[a] | −4.6 | −4.7[a] | 3.4 | 4.0 | 0.67 | – | 0.60 | 0.43 | 0.43 | 0.45 | 9.0 | 0.11 | 0.00 |
| AV | – | 7.3 | – | 6.7 | 6.1 | 0.56 | – | 0.49 | 0.39 | 0.41 | 0.43 | Σ = 92 | – | – |

[a] 12/1/2011–12/13/2011.
[b] LR for loggers from January to May was based on measured LR from other months. See text for details.

sured LR in December was the minimum LR of the year, and that the measured LR in June was the maximum LR of the year. Then, LR for January was set equal to LR for November, LR for February was set equal to LR observed in October, and so forth. Evaporation from January to May accounts for 12% of annual evaporation (Table 2), which minimizes the impact of those months on the flux-weighted variable means used in the isotope model. A second set of monthly LR was taken from a time series of MODIS land surface temperature (LST) imagery (MOD11A1) from 2003 to 2011 and a digital elevation model from the Shuttle Radar Topography Mission (SRTM). Uncertainty in $E/I$ introduced by uncertainty in LR was quantified (see Section 3.4).

Measurements of $h$ at Tso Moriri were only available for two months (July and August, 2011), so the annual time series of $h$ at the lakes was determined in three ways. First, we assumed that mean monthly $h$ at Tso Moriri and Tso Kar was equal to the mean monthly $h$ measured at Leh from 2000 to 2006 (Table 2). Second, $h$ at each lake was taken as $h$ at Leh corrected by the observed difference between $h$ at Leh and $h$ at Tso Moriri weather station in July and August ("$h$ TM corr.", Table 2). Third, $h$ was calculated using data from the global gridded dataset Modern-Era Retrospective Analysis for Research and Applications (MERRA) from the Global Modeling and Assimilation Office (GMAO) (tavgM_2d_slv_Nx), which as a cell size of 0.67° longitude by 0.5° latitude. The GMAO data served several purposes. First, they helped assess the variability of $h$ over different averaging periods (e.g. 2011 only, 2000–2006, 1979–2012). This is important because the meteorological data for Leh were only available for 2000–2006, but $h$ values from that period were used to represent the long-term mean. Second, the GMAO data on $h$ were used as input to the isotopic model directly to test for the effect of using global gridded data on $E/I$. This application assumes that $h$ was uniform over a grid cell, which may not be true in a mountainous environment. In our particular study area, the mean elevation in the GMAO grid cells was similar to the elevation of the lakes. While $h$ can also be calculated by assuming that the vapour pressure equals the saturation vapour pressure at the daily minimum $T_a$, this was not a reasonable assumption for the region given its low annual precipitation and overestimated $h$ by an average of 9% and up to 33% at Leh during the months with the highest evaporation rates.

### 3.3. Isotope analysis: Laboratory methods

Stable isotope analysis of water samples was performed on a DLT-100 liquid water isotope analyzer (LWIA) (Los Gatos Research (LGR) Inc, CA, USA) coupled to a LC PAL autosampler system (CTC Analytics AG, Zwingen, Switzerland) at San Diego State University. An aliquot of 0.5 ml water was pipetted from each unknown sample and loaded in a 2 mL sample vial before analysis. Five laboratory-working references, traceable to the V-SMOW scale, were included in each run and used to calibrate field samples. Post data analysis was performed using LGR's LWIA data software. The analytical precision and accuracy of our measurements was reported to the IAEA 2011 Proficiency Test on the Determination of Stable Isotope in Water. We report the accuracy as 0.1(±0.07)‰ for $\delta^{18}O$ and 0.6(±0.4)‰ for δD. Our day-to-day precision is reported as 0.25‰ for $\delta^{18}O$ and 1.0‰ for δD.

### 3.4. Uncertainty analysis

The main meteorological variables that were not directly measured over a full annual cycle included the temperature lapse rate (LR) and $h$. We analyzed the sensitivity of $E/I$ to the methods used to calculate each variable (see 3.2.2). For the sensitivity analysis, we used two values for LR (loggers and MODIS) and three values for $h$ (Leh, corrected, and GMAO). The main isotopic input variable

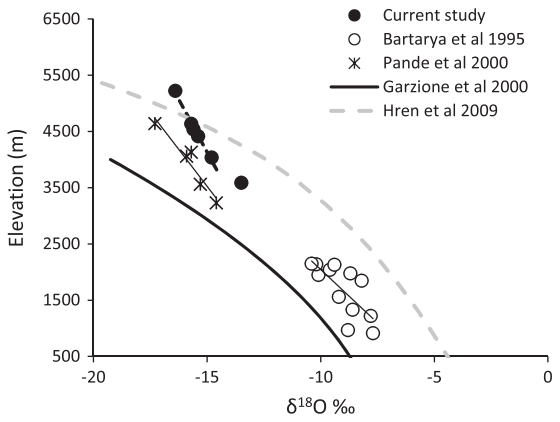


**Fig. 3.** Relationship between elevation and isotopic composition of stream water samples in the current study and in other studies. The line from Garzione et al. (2000) is a best fit-regression line for samples taken in Nepal. The line from Hren et al. (2009) is the output of a thermodynamic model that fit the data from a regional survey across the Himalaya.

that may vary in time is the isotopic composition of inflow ($\delta_I$), for which we had one observation in time. For $\delta_I$, we first used the observed relationship between elevation and inflow (Fig. 3) to estimate the isotopic composition of inflow at each lake given its elevation. While the mean elevation of the watershed or the hypsometric mean elevation of the watershed has been used to model the relationship between elevation and inflow (Hren et al., 2009), the mean watershed elevation did not correlate with isotopic composition in our sites and so the elevation of the sample site was used instead. A second estimate of the isotopic composition of inflow may be derived from the intersection of the evaporation line from the lakes with the global meteoric water line (GMWL) from Rozanski et al. (1993) (Fig. 4). The equation for the evaporation line was $\delta D = -35 + 5.87\ \delta^{18}O$, which intersects the GMWL at $\delta^{18}O = -19.1‰$ and $\delta D = -144.5‰$. For several lakes, using this predicted value of $\delta_I$ gave unreasonable values of $E/I$, including values much greater than 1.0 and less than zero. $E/I$ can be less than zero if the estimate of $\delta^*$ is more negative than the observed isotopic composition of the lake. Due to the unreasonable values of $E/I$ that resulted from using the predicted value of $\delta_I$, we used the observed elevation–isotope relationship (Fig. 3) to estimate $\delta_I$ at each lake.

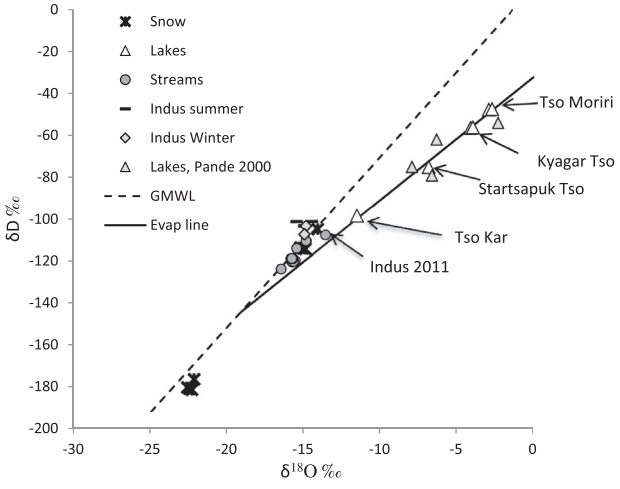


**Fig. 4.** $\delta^{18}O$ versus δD for stream water, snow, and lake water in the current study, with additional samples from the Indus River mainstem in Pakistan (Karim and Veizer, 2002) and samples of the same four lakes taken in 1991 (Pande et al., 2000). The global meteoric water line (GMWL) used here has a slope of 8.13 and an intercept of 10.8 (Rozanski et al., 1993).

In order to test for the possible impact of snowmelt runoff on lake isotopic composition and E/I, we used a simple water balance and satellite-derived snow cover to estimate the isotopic composition of the lakes before snowmelt:

$$\delta_{L.Pre} = \frac{\delta_{L.Pst} V_{L.Pst} - \delta_I V_I}{V_{L.Pre}} \quad (4)$$

where $V_L$ is the volume of water in the lake and Pre and Pst indicate pre-melt and post-melt. The lake samples were collected after the main period of snowmelt (June 2011, Fig. 2), so the observed $\delta^{18}O$ in June 2011 was used for $\delta_{L.Pst}$. The volume of the lake pre-melt was calculated from recent estimates of lake surface area (2013) and the depth values from Hutchinson (1937). The volume of inflow due to snowmelt from the beginning of snowmelt to the time of sampling ($V_I$) is calculated in two ways, first as:

$$V_I = C_{sn}(\Delta A_{SC})SWE \quad (5)$$

where $C_{sn}$ is the snowmelt runoff coefficient, $\Delta A_{SC}$ is the change in snow covered area in the watershed from the time of maximum snow cover in the winter to the time of sampling, and SWE is the snow water equivalent of the snowpack that melts, assumed to be the sum of mean monthly precipitation between December and April at Leh (51 mm, Table 2), the period of increasing snow cover (Fig. 2). $\Delta A_{SC}$ for the year of sampling (2011) was taken from the MODIS snow cover product (MOD10A2), which is at 1 km and 8-day resolution. $C_{sn}$ was taken from other studies in the Himalaya (Panday et al., 2014) with a similar elevation range (4000–5500 m, average $C_{sn} = 0.59$). Eq. (5) assumes minimal melt from snow covered areas that did not melt completely between the start of the decrease in snow cover and the time of measurement (June), and therefore may underestimate the volume of snowmelt. $A_{sc}$ in June was 0.2 of the watershed area, and the monthly mean temperature at elevations with snow cover in June (>5500 m), estimated from the long-term mean $T_a$ at Leh and LR (Table 2) was less than 0 °C from March to May, suggesting minimal melt at those high elevations.

$V_I$ was also approximated using a degree-day method (Rango and Martinec, 1995) and 8-day MODIS $A_{SC}$:

$$V_I = \sum_{i=1}^{n}\sum_{j=1}^{k} 8C_{sn}(A_{SCi,j})a_n T_{ai,j} \quad (6)$$

where $i$ is an index of $n$ 8-day periods corresponding to MODIS $A_{sc}$ measurements, $j$ is an index of $k$ elevation zones, $a_n$ is the degree-day factor (mm $d^{-1}$ °$C^{-1}$) and $T_{ai,j}$ is mean air temperature for the 8-day period in elevation zone $j$, estimated using the historical temperature data from Leh (2000–2006) and LR from the loggers (Table 2). $a_n$ was assumed to be 4 mm $day^{-1}$ °$C^{-1}$, which is the value for late-season melt (mid-May) in the Sierra Nevada (Rango and Martinec, 1995), and likely represents an upper-bound value. Elevation zones were created using 500 m increments.

There are many uncertainties in the snowmelt models represented by Eqs. (5) and (6), and the input data ($T_{ai,j}$) were not available for the year when the water samples were collected. $T_{ai,j}$ is also best determined at a daily time-step, while only monthly data was available. Given those uncertainties, the objective here was to perform a simple sensitivity analysis of the possible magnitude of seasonal fluctuations in the isotopic composition and computed $E/I$ of the lakes, using some plausible estimates of $V_I$. We used upper-bound values of the degree-day factor ($a_n$) to provide the largest plausible values of $V_I$, which results in an upper-bound estimate of the impact of snowmelt inflow on isotopic composition and the resulting $E/I$. If seasonal effects are estimated to be large, future work could more completely account for runoff magnitude, timing and impact on the lake water balance and isotopic composition, perhaps using more detailed satellite and meteorological data (Bookhagen and Burbank, 2010).

$\delta_{L.Pre}$ was estimated for Tso Moriri, Kyagar Tso, and the combined Tso Kar-Startsapuk Tso pair using Eqs. 4–6. Startsapuk Tso drains into Tso Kar, so accounting for runoff-induced changes in isotopic composition would require an estimate of the flow between the two lakes. In order to simplify the analysis, the two lakes were combined, using the volume-weighted $\delta^{18}O$ as the estimate of $\delta_{L.Pst}$.

## 4. Results

### 4.1. Elevation and deuterium excess

The isotopic composition of stream water varied linearly with the elevation of the sample location (Fig. 3, Table 3), which reflects rain out of the heavier isotope at lower elevations. Linear regression models were used to estimate slope of the isotope–elevation relationship for both the 2011 dataset and for the dataset of Pande et al. (2000) who sampled some of the same streams (Fig. 3, Table 4). The lakes all had similar elevations (4535–4736 m), so the modelled isotopic composition of inflow ($\delta_I$) based on the linear regressions was similar for all lakes.

The isotopic composition of stream and snow samples plot on the global meteoric water line (GMWL) (Fig. 4). Snow that fell during a storm in early June had much lighter isotopic composition than snow on the ground. The deuterium excess ($d$) of the stream samples, excluding the Indus River, averaged + 7.5‰ with a range from 4.9‰ to 9.6‰ (Table 3). The Indus River had lower $d$ (+1‰) than the other samples, perhaps due to some evaporative effects as reflected in the single sample taken in June 2011 (Fig. 4).

### 4.2. Evaporation fraction

The isotopic composition of lake water showed strong evidence of evaporative fractionation (Fig. 4). All points plot along a single local evaporative line (LEL), with a slope of 5.9, which is in the range of commonly observed values (4–7) (Gibson et al., 2002).

$E/I$ predicted from the isotopic model ranged from 0.16 to 1.20 (Table 5) depending on the lake and input values of $h$. The two deepest lakes (Tso Moriri and Kyagar Tso) had higher $E/I$ than the two shallow lakes. Despite the fact that Startsapuk Tso drains into Tso Kar, it had a higher $E/I$ than Tso Kar. A surficial channel links the two lakes but its role in their annual water balance of Tso Kar is not known. In addition to inflow from Startsapuk Tso, Tso Kar also receives inflow from tributaries to the north and south, which have a larger drainage area than the watershed draining to Startsapuk Tso. Inflow from these watersheds should be unaffected by evaporation and may account for the lower $E/I$ at Tso Kar compared with Startsapuk Tso.

$E/I$ estimates were sensitive to $h$, particularly for high $E/I$ values (Table 5). Using the uncorrected $h$ from the low elevation station (Leh), which were the highest $h$ estimates tested, resulted in higher $E/I$, with $E/I$ greater than 1 for one lake (Table 5). $E/I$ calculated using $h$ corrected to data from the Tso Moriri weather station were higher than $E/I$ calculated using $h$ from the GMAO data (Table 5). The results suggest that correct estimation of $h$ is critical for estimating $E/I$ in arid regions like the western Himalaya, and that global datasets like GMAO-MERRA may provide input data with sufficient accuracy. The sensitivity of $E/I$ to $h$ did not change the overall finding that evaporation represents more than half of inflow at the deeper lakes and less than half the inflow at the shallow lakes.

$E/I$ was not sensitive to the value of LR used in the model, and differences between $E/I$ for the two LR methods was less than 5%

**Table 3**
Mean isotopic composition and sampling locations of snow, stream water, and lake water.

| | Elevation at sampling site (m) | Latitude | Longitude | $\delta^{18}O$‰ | δD‰ | D excess |
|---|---|---|---|---|---|---|
| *Snow* | | | | | | |
| Tso Moriri pass | 4779 | 33.15697 | 78.35817 | −15.0 | −113.7 | +6 |
| Tso Moriri snowfall | 4543 | 32.96987 | 78.26384 | −22.4 | −180.4 | −2 |
| Taglangla Pass 1 | 5330 | 33.50769 | 77.76962 | −14.0 | −104.6 | +8 |
| Taglangla Pass 2 | 4906 | 33.48506 | 77.81180 | −22.1 | −176.0 | +1 |
| *Streams* | | | | | | |
| 1 Tso Moriri inflow 1 | 4637 | 33.06982 | 78.27538 | −15.7 | −118.6 | +7 |
| 2 Tso Moriri inflow 2 | 4535 | 33.02215 | 78.27179 | −15.6 | −119.9 | +5 |
| 3 North of Tso Moriri | 4414 | 33.22758 | 78.37143 | −15.4 | −113.6 | +10 |
| 4 Tributary of Indus | 4035 | 33.35787 | 78.35414 | −14.8 | −110.2 | +8 |
| 5 Spring at Taglangla | 5223 | 33.51951 | 77.79467 | −16.4 | −123.5 | +8 |
| 6 Indus mainstem | 3586 | 33.69571 | 77.97470 | −13.5 | −107.4 | +1 |
| *Lakes and (max. depth)*[a] | | | | | | |
| Tso Moriri, $N = 2$ (75.5 m) | 4535 | 32.96770 | 78.29675 | −2.8 | −47.6 | −25 |
| Kyagar Tso (21.2 m) | 4736 | 33.12340 | 78.30348 | −4.0 | −56.2 | −24 |
| Startsapuk Tso (2 m) | 4640 | 33.25591 | 78.05392 | −6.8 | −75.1 | −21 |
| Tso Kar (~2 m) | 4640 | 33.31855 | 78.03497 | −11.5 | −98.3 | −6 |

[a] Maximum depth data are from Hutchinson (1937).

**Table 4**
Regression parameters for $^{18}O$ and D in stream water as a function of sampling elevation ($z$ in m). The regressions for this study exclude the Indus River point.

| | $^{18}O$ | Std error | $R^2$ | $D$ | Std error | $R^2$ |
|---|---|---|---|---|---|---|
| This study | −0.00133$z$−9.50 | 0.07 | 0.99 | −0.0113z−65.36 | 2.3 | 0.81 |
| Pande et al. (2000) | −0.00194$z$−8.01 | 0.50 | 0.78 | −0.0134z−58.59 | 7.0 | 0.42 |

**Table 5**
Evaporative fractions ($E/I$) using either $^{18}O$ or D for the four sampled lakes given different values of relative humidity ($h$). h.GMAO corresponds to the mean monthly $h$ over 1979–2012 from the GMAO-MERRA dataset at Tso Moriri. The lapse rate was from the temperature loggers (Table 2). See Section 3.2.2 for details on the methods. $\Delta$ is the difference in $E/I$ between the models using $^{18}O$ and the models using D.

| | Mean annual $h$ | $E/I$ | | |
|---|---|---|---|---|
| | | $^{18}O$ | D | $\Delta$ |
| *Tso Moriri* | | | | |
| h Leh | 0.56 | 1.18 | 1.20 | −0.02 |
| h TM corrected | 0.49 | 0.87 | 0.83 | 0.04 |
| h.GMAO | 0.42 | 0.72 | 0.66 | 0.06 |
| *Kyagar Tso* | | | | |
| h Leh | 0.56 | 0.98 | 0.97 | 0.01 |
| h corrected | 0.49 | 0.76 | 0.71 | 0.05 |
| h.GMAO | 0.42 | 0.64 | 0.57 | 0.07 |
| *Tso Kar* | | | | |
| h Leh | 0.56 | 0.21 | 0.20 | 0.01 |
| h corrected | 0.49 | 0.20 | 0.18 | 0.02 |
| h h.GMAO | 0.42 | 0.19 | 0.16 | 0.03 |
| *Startsapuk Tso* | | | | |
| h Leh | 0.56 | 0.58 | 0.53 | 0.05 |
| h corrected | 0.49 | 0.50 | 0.44 | 0.06 |
| h.GMAO | 0.42 | 0.45 | 0.38 | 0.07 |

for all lakes for both $^{18}O$ and D. $E/I$ calculated with LR derived from the temperature loggers are presented in Table 5. The results suggest that MODIS LST imagery can be used to calculate lapse rates with sufficient accuracy for modelling $E/I$ in high elevation lakes in arid regions.

$E/I$ calculated using $^{18}O$ were similar to $E/I$ calculated using D; the absolute difference between $E/I$ calculated using each isotope was less than or equal to 0.07 when using the corrected and GMAO humidity values (Table 5). Importantly, use of the laboratory $\varepsilon_K$ for D (Gibson and Edwards, 2002) resulted in very different values of $E/I$ compared to $E/I$ from $^{18}O$; the apparent value of $\varepsilon_K$ based on field observations by Zuber (1983) resulted in a much closer match between $E/I$ from the two isotopes, and should be used in future work in regions with low humidity.

The estimate of snowmelt volume ($V_I$, Table 6) yielded reasonable values for the net increase in lake water levels during the snowmelt period (0.04–0.67 m). The model where SWE is assumed to be equal to SWE at Leh during the winter (Eq. (5)) yielded larger estimates of $V_I$ than the degree-day model (Eq. (6)). The impact of the snowmelt inflow on the isotopic composition and $E/I$ was very small for the largest two lakes (Tso Moriri and Kyagar Tso), and moderate for Tso Kar plus Startsapuk Tso pair (Table 6). The larger impact of seasonal inflow on the isotopic composition and $E/I$ in the shallow lakes is consistent with their large watershed area to lake area ratio.

## 5. Discussion

### 5.1. Isotopic composition in regional context

The deuterium excess ($d$) of stream water (+7.5‰) was similar to d in precipitation from the summer monsoon (+8‰) (Karim and Veizer, 2002), suggesting that the dominant source of moisture for precipitation in the study area at the time of sampling was the Indian summer monsoon, rather than the winter westerlies, which have higher $d$ (~22‰) (Karim and Veizer, 2002). Compared to the Tso Moriri stream samples, headwater tributaries of the Indus River to the west in Pakistan show higher d values, (+12 to +22‰, average +14.7‰), and the mainstem of the Indus has a discharge-weighted average $d$ of +18‰, indicating the importance of westerly moisture sources west of our study site (Karim and Veizer, 2002). Some snow samples collected in 2011 had very low $d$ (−2‰), which was within the range observed in stream water in the Upper Yarlung Tsangpo basin, southeast of the Tso Moriri study area (−3‰ to 12‰) (Hren et al., 2009), and in precipitation at a site approximately 200 km from the study area (80°E, 32.5°N, 4279 m, $d$ range −10 to +21‰, mean $d$ ~10‰) (Tian et al., 2007). Below-cloud secondary evaporation during the descent of raindrops or ice crystals, an effect common to precipitation events in dry environments, is likely the reason behind these low d values (Stewart, 1975), and may complicate the use of d for

**Table 6**
Estimates of seasonality of isotopic composition due to snowmelt runoff. Calculations assume $C_{sn}$ of 0.59 (Eqs. (5) and (6)) and snow water equivalent of 51 mm (Eq. (5)).

| | Tso Moriri | Kyagar Tso | Tso Kar + Startsapuk Tso |
|---|---|---|---|
| $V_{L.Pre}$ (MCM) | 7975 | 75 | 43 |
| $V_I$ (MCM) | | | |
| Eq. (5) | 36 | 1 | 11 |
| Eq. (6) | 33 | 0.3 | 1.2 |
| $\Delta z$ (m) | | | |
| Eq. (5) | 0.24 | 0.22 | 0.67 |
| Eq. (6) | 0.22 | 0.04 | 0.05 |
| $\Delta A_{SC}$ (fraction) | 0.50 | 0.56 | 0.70 |
| $\delta_{L.Pst}$ (observed) | −2.8 | −4.0 | −11.0 |
| $\delta^{18}O_{Pre}$ (modelled) | | | |
| Eq. (5) | −2.7 | −3.8 | −9.9 |
| Eq. (6) | −2.7 | −4.0 | −10.9 |
| $E/I$ using observed $\delta^{18}O_{Pst}$ | 0.87 | 0.76 | 0.22 |
| $E/I$ using modelled $\delta^{18}O_{Pre}$ | | | |
| Eq. (5) | 0.88 | 0.78 | 0.29 |
| Eq. (6) | 0.88 | 0.76 | 0.23 |

moisture source identification. Overall, our results are consistent with other regional surveys of precipitation and streamflow, with similar $d$ values that suggest dominance of monsoonal moisture in precipitation and streamflow (Hren et al., 2009; Tian et al., 2007).

The dominance of the monsoon as a moisture source in our study streams contrasts with expectations based on the importance of winter snow in annual precipitation at Leh, which should have an isotopic signature from westerly air masses (Karim and Veizer, 2002). The Tso Moriri study region is in the transition zone between summer and winter-dominated precipitation regimes mapped by Bookhagen and Burbank (2010); the d values suggest that Tso Moriri is in the region dominated by summer precipitation and monsoon moisture sources. Our water sampling occurred after a period of snowmelt, suggesting that water held in snow from the westerlies may have melted and runoff prior to sampling, though groundwater recharge would likely delay some of the release of the melted water into the stream until at least the sampling date. Snow that fell just before and during the field campaign had $d$ values close to the $d$-excess of a monsoon source, suggesting that monsoonal precipitation can occur as snow.

### 5.2. Elevation effects on stream isotopic composition

The $\delta^{18}O$ composition of stream water correlated closely with elevation in the study area (Fig. 3). The slope of the $\delta^{18}O$–elevation relationship, excluding the Indus River sample (−0.133‰/100 m) was similar to that observed at low elevations (915–2150 m) in Kumaun Lesser Himalaya south of Tso Moriri (−0.146‰/100 m) (Bartarya et al., 1995), but lower than observed for the low-elevation headwaters of the Ganges (30–31°N, 78–79°E, 300–3000 m, −0.19‰/100 m) (Ramesh and Sarin, 1992) (Fig. 3) and lower than observed in the central and eastern Himalaya and Tibetan Plateau (−0.29‰/100 m) and Nepalese Himalaya (−0.29‰/100 m) (Garzione et al., 2000). The six samples of stream water from Pande et al. (2000), which included some of the same streams sampled in 2011, result in higher slopes of the elevation–$\delta^{18}O$ relationship (−0.194‰/100 m, Fig. 3, Table 4) compared to our observation (−0.133‰/100 m).

The $\delta^{18}O$ in the 2011 samples fell around the prediction of Hren et al. (2009) who used a thermodynamic model to predict the $\delta^{18}O$–elevation relationship (Fig. 3), but the model predicted a higher slope (−0.53‰/100 m) than was observed (−0.133‰/100 m).

The lack of a systematic trend in the slope of the elevation–isotope relationship contrasts with the thermodynamic model (Hren et al., 2009) and with regional surveys of stream water in the eastern and central Himalaya, which show an increase in the slope with elevation (Garzione et al., 2000; Hren et al., 2009), corresponding to a flattening of the $\delta^{18}O$–elevation relationship in Fig. 3. The relatively low slope of the $\delta^{18}O$–elevation relationship in the Tso Moriri area may be due to differences in $h$ and LR (Hren et al., 2009). The low scatter in the $\delta^{18}O$-elevation relationship at high elevations in the Tso Moriri area also contrasts with the weak $\delta^{18}O$–elevation relationships above 3–4 km elevation observed by Pande et al. (2000). The scatter around the $\delta^{18}O$–elevation relationship in the data from Pande et al. (2000) may be due in part to spatial variations in isotopic composition, rather than to a change in or weakening of the elevation–isotope relationship with increasing elevation. The samples from Pande et al. (2000) that are within and near our study site have a similar $\delta^{18}O$–elevation relationship as observed in our samples (Fig. 3), suggesting that regional variation in isotopic composition due to vapour origin, $h$ or LR may result in an apparent weakening of the $\delta^{18}O$–elevation gradient with elevation, and that strong $\delta^{18}O$–elevation relationships occur at local scales.

### 5.3. E/I values and comparison with previous surveys of the region

The modelled values of $E/I$ were insensitive to the temperature lapse rate, but were sensitive to different values of $h$, particularly for high values of $E/I$. This suggests that constraining the value of $E/I$ using isotopic methods may be limited by the availability of data on $h$ in arid regions. Global gridded data (GMAO-MERRA) provided reasonable values of $h$ and $E/I$, despite the large range of elevations covered in a single GMAO cell, suggesting that global gridded data could be further explored for its ability to provide $h$ for isotopic models of $E/I$. $E/I$ was insensitive to modelled seasonal changes in the isotopic composition of the lakes caused by inflow of snowmelt, though there is significant uncertainty in the estimates of snowmelt runoff volume and its isotopic composition. Further research could explore the seasonality of the isotopic composition, though our preliminary calculations suggest that the seasonal effects do not change isotopic composition or the resulting $E/I$ values significantly.

The isotopic composition and $E/I$ values for the 2011 samples and the 1991 samples (Pande et al., 2000) were similar for Startsapuk Tso and Kyagar Tso, except for $^{18}O$ for Kyagar Tso, which gave a higher $E/I$ compared to both our study and to $E/I$ calculated using D from 1991 (Table 7). Tso Moriri (Tso Kar) had lighter (heavier) isotopic values in 1991 compared to 2011 (Table 7), and the resulting $E/I$ were smaller (larger) in 1991 compared to 2011. $E/I$ calculated using the 1991 samples differed according to which isotope was used ($^{18}O$ or D) at Kyagar Tso and Tso Kar; removing the estimate of $E/I$ calculated using $^{18}O$ from 1991 results in a closer match in $E/I$ between 1991 and 2011. The lighter isotopic composition at Tso Kar in June 2011 compared to August 1991 could be due to inflow from snowmelt runoff, though one might expect the same phenomenon at the nearby Startsapuk Tso, which showed no such interannual variability. The large difference in isotopic composition at Tso Moriri between 1991 and 2011 could be due to differences in runoff dilution, depth of sample if isotopic composition is not uniform with depth, location of the sample, or differences in analytical techniques and their precision. Isotopic composition of large lakes can differ with distance to shore, with less evaporative fractionation observed near the shoreline due to inflow of water from surface or subsurface sources that have low evaporative signatures. The Tso Moriri samples from 2011 were taken from the centre of the lake, while the 1991 samples were taken from the

**Table 7**
Comparison of isotopic values and *E*/*I* from this study and from the same lakes from Pande et al. (2000), using corrected h to calculate *E*/*I* (Table 2). The numbers in parentheses to the right of the lake names indicate the maximum lake depth.

| | $\delta^{18}O$‰ | | δD‰ | |
|---|---|---|---|---|
| | This study | Pande et al. (2000) | This study | Pande et al. (2000) |
| *Streams* | | | | |
| Tso Moriri inflow 2 | −15.6 | −17.3 | −119.9 | −124 |
| *Lakes* | | | | |
| Tso Moriri (75.5 m) | −2.8 | −6.3 | −47.6 | −62 |
| Kyagar Tso (21.2 m) | −4.0 | −2.3 | −56.2 | −54 |
| Startsapuk Tso (2 m) | −6.8 | −7.9 | −75.1 | −75 |
| Tso Kar (~1–2 m) | −11.5 | −6.6 | −98.3 | −79 |
| | *E*/*I* from $\delta^{18}O$‰ | | *E*/*I* from δD‰ | |
| | This study | Pande et al. (2000) | This study | Pande et al. (2000) |
| Tso Moriri (75.5 m) | 0.85 | 0.63 | 0.83 | 0.64 |
| Kyagar Tso (21.2 m) | 0.74 | 1.16 | 0.71 | 0.81 |
| Startsapuk Tso (2 m) | 0.49 | 0.52 | 0.44 | 0.49 |
| Tso Kar (~1–2 m) | 0.19 | 0.63 | 0.18 | 0.43 |
| Mean deep lakes | 0.79 | 0.87 | 0.78 | 0.74 |
| Mean shallow lakes | 0.33 | 0.56 | 0.32 | 0.46 |

lake shore, which could contribute to the observed differences in isotopic composition. For now, we note that there appears to be temporal variability in isotopic composition at some lakes, but the sources of the variability are not known.

Despite differences in *E*/*I* values calculated using the data from 1991 and 2011, together the results suggest that deeper lakes have higher *E*/*I* than shallow lakes (Table 7). The two deep lakes had *E*/*I* greater than or equal to 0.63 for all methods and sampling times, while the shallow lakes had *E*/*I* less than or equal to 0.63 for all methods and sampling times. The mean *E*/*I* for the two deep lakes was greater than the mean *E*/*I* from the two shallow lakes (Table 6). The hydrological significance of this difference in *E*/*I* by lake depth is discussed in Section 5.4.

### 5.4. Significance of evaporation for regional hydrology

The *E*/*I* values from the isotope measurements from 2011 suggest that the deepest lakes are in relatively "closed" basins that lose most of their inflow to evaporation (77–87%, using h.TM.corrected and LR from loggers) and relatively little to outflow (13–23%). The shallow lakes have lower *E*/*I* (18–50%) and lose a significant fraction of their inflow to outflow (50–82%), presumably to groundwater recharge given the lack of visible surface outflow. This pattern held in both 1991 and 2011, with somewhat less contrast between shallow and deep lakes in the 1991 survey.

The difference in the *E*/*I* values between the deep and shallow lakes corresponds with differences in the ratio of lake volume to watershed area ($V_L$:$A_w$, Table 1). The shallow depth and low $V_L$:$A_w$ of the Tso Kar-Startsapuk Tso pair may correspond with a lower hydraulic residence time, and therefore a lower total evaporative enrichment, which is consistent with a larger loss to groundwater in the annual hydrological budget. A more complete hydrologic budget of the lakes would be required to calculate residence times and to clarify the relationship between evaporative isotopic enrichment, lake morphology, geology, and water residence time.

The contribution of evaporatively enriched water to discharge in larger basins downstream of the study area can be assessed using isotopic observations of the Indus River basin, which includes our study area. Isotopic values that fall on the evaporation line would indicate a contribution of evaporatively enriched water, either from natural lakes or reservoirs. This contribution could be particularly important during periods of low discharge in winter and spring.

Isotopic values were reported for the Indus River at 69 locations, in the winter and again in the summer of 1994–1995, and once per month from March 1994 to February 1995 at one location downstream in the arid lowlands of Pakistan (Sukkur Barrage) (Karim and Veizer, 2002). The isotopic values in the headwaters of the Indus did not indicate evaporative enrichment in either the summer, when discharge is highest, or in the winter during low flow (Fig. 4). Water from the Indus had higher $^{18}O$ abundance during the winter, but this was attributed to changes in the source of precipitation and runoff, rather than to evaporative enrichment of the source waters (Karim and Veizer, 2002). We conclude that water with a strong evaporative isotopic enrichment, like those observed in two of our four studied lakes, plays a limited role in maintaining streamflow to the mainstem of the Indus River in both dry and wet seasons, though we suspect that evaporatively enriched water is important for maintaining discharge in some smaller watersheds.

The large *E*/*I* observed in the two deep lakes in the Tso Moriri area contrasts with results from one of the largest lakes in the Tibetan Plateau (Nam Co), which lost more than half of its inflow to groundwater seepage (Zhou et al., 2013). The mean depth of the lakes is similar (45.6 m at Nam Co (Zhang et al., 2011), 55 m at Tso Moriri), so the difference between Nam Co and the Tso Moriri lakes may be due to a combination of climate and geological setting. The Nam Co watershed has higher annual precipitation (610 mm) than the Tso Moriri watershed (92–270 mm), and is located on an extensive fault zone (Zhou et al., 2013). The relationship between *E*/*I* and lake depth in the Tso Moriri area suggests that there may be a systematic difference in *E*/*I* related to a combination of watershed and lake characteristics. The large spatial variability in the observed evaporative fractions, even for lakes in topographically closed basins, also suggest that there is large uncertainty in the role of high elevation lakes in the hydrology of Himalayan river systems. Application of the isotopic techniques demonstrated here could contribute towards a more complete understanding of the role of lakes in the water budget of the Himalaya. A regional sampling of the isotopic composition of lake water in the Himalaya would help establish the relationship between the evaporative fraction, lake morphology, geology, climate and watershed characteristics.

### 5.5. Implications for regional monitoring and comparisons

Modelled *E*/*I* was sensitive to *h*, especially for high *E*/*I* values (Table 5). *E*/*I* was less sensitive to LR, though our two sets of values for LR were not very different (Table 2). The sensitivity analysis suggests that monitoring of *h*, if only for a short period of time, would be helpful to constrain *E*/*I* estimates for lakes in the Himalaya. *E*/*I* calculated using *h* from local and global datasets suggest that global data like the gridded GMAO-MERRA datasets may be used to estimate *h*, particularly for relatively low values of *E*/*I* (e.g. $E/I < 0.5$), though the validity of applying the global datasets to a particular location should be validated with ground-based meteorological measurements.

## 6. Conclusion

This study documented that evaporation comprises the majority of inflow to two deep lakes in the arid western Himalaya, indicating near complete basin closure to outflow. Two shallow lakes showed significant loss to outflow through groundwater, but large river systems did not show a strong signature of evaporative enrichment, and therefore likely have limited dependence on recharge from lakes experiencing large evaporation loss. Evaporatively enriched lakes may play a role in maintaining low flow

in smaller drainages, but that effect is dampened at the scale of the mainstem of the Indus River. A close relationship was observed between elevation and isotopic composition, consistent with rain out of heavier isotopes at lower elevations. Both stream water and snow showed deuterium-excess signatures of a monsoon moisture source. Lakes in hydrologically closed basins may be highly sensitive to climate change, since their storage cannot be maintained through a reduction in outflow (Jones et al., 2001). The results here suggest that some lakes at high elevation in the Himalaya may be hydrologically closed and therefore sensitive to climate change. Isotopic analysis can help identify sensitive lakes in the Himalaya and elsewhere.

## Acknowledgements

This project was funded by a grant from the Worldwide Fund for Nature-India (WWF-India). C.-T Lai was supported by the U.S. National Science Foundation, Division of Atmospheric and Geospace Sciences under Grant Number AGS-0956425. Many thanks to the WWF staff for help with the field campaign. Two anonymous reviewers provided valuable input that improved the analysis and manuscript.

## Appendix A. Supplementary material

Supplementary data associated with this article can be found, in the online version, at http://dx.doi.org/10.1016/j.jhydrol.2014.12.023.

## References

Bagati, T.N., Thakur, V.C., 1993. Quaternary basins of Ladakh and Lahaul-Spiti in northwestern Himalaya. Curr. Sci. 64, 898–903.
Bartarya, S.K., Bhattacharya, S.K., Ramesh, R., Somayajulu, B.L.K., 1995. $\delta^{18}O$ and $\delta D$ systematics in the surficial waters of the Gaula river catchment area, Kumaun Himalaya, India. J. Hydrol. 167, 369–379.
Bhattacharyya, A., 1989. Vegetation and climate during the last 30,000 years in Ladakh. Palaeogeogr. Palaeoclimatol. Palaeoecol. 73, 25–38. http://dx.doi.org/10.1016/0031-0182(89)90042-4.
Bookhagen, B., Burbank, D.W., 2010. Toward a complete Himalayan hydrological budget: spatiotemporal distribution of snowmelt and rainfall and their impact on river discharge. J. Geophys. Res. 115, F03019. http://dx.doi.org/10.1029/2009jf001426.
Bookhagen, B., Thiede, R.C., Strecker, M.R., 2005. Late quaternary intensified monsoon phases control landscape evolution in the northwest Himalaya. Geology 33, 149–152.
Bullock, A., Acreman, M., 2003. The role of wetlands in the hydrological cycle. Hydrol. Earth Syst. Sci. 7, 358–389.
Delclaux, F., Coudrain, A., Condom, T., 2007. Evaporation estimation on Lake Titicaca: a synthesis review and modelling. Hydrol. Process. 21, 1664–1677.
Dincer, T., 1968. Use of oxygen 18 and deuterium concentrations in water balance of lakes. Water Resour. Res. 4, 1289–1306.
Dunne, T., Leopold, L.B., 1978. Water in Environmental Planning. W.H. Freeman and Company, New York.
Garzione, C.N., Quade, J., DeCelles, P.G., English, N.B., 2000. Predicting paleoelevation of Tibet and the Himalaya from $\delta^{18}O$ vs. altitude gradients in meteoric water across the Nepal Himalaya. Earth Planet. Sci. Lett. 183, 215–229. http://dx.doi.org/10.1016/S0012-821X(00)00252-1.
Gibson, J.J., Edwards, T.W.D., 2002. Regional water balance trends and evaporation–transpiration partitioning from a stable isotope survey of lakes in northern Canada. Global Biogeochem. Cycles 16, 10-1–10-14. http://dx.doi.org/10.1029/2001GB001839.
Gibson, J.J., Prepas, E.E., Mceachern, P., 2002. Quantitative comparison of lake throughflow, residency, and catchment runoff using stable isotopes: modelling and results from a regional survey of Boreal lakes. J. Hydrol. 262, 128–144.
Gonfiantini, R., 1986. Environmental isotopes in lake studies. In: Fritz, P., Fontes, J.-C. (Eds.), Handbook of Environmental Isotope Geochemistry, The Terrestrial Environment, vol. 2. Elsevier, Amsterdam, The Netherlands, pp. 113–168.
Hedrick, K.A., Seong, Y.B., Owen, L.A., Caffee, M.W., Dietsch, C., 2011. Towards defining the transition in style and timing of quaternary glaciation between the monsoon-influenced Greater Himalaya and the semi-arid Transhimalaya of Northern India. Quat. Int. 236, 21–33. http://dx.doi.org/10.1016/j.quaint.2010.07.023.
Hren, M.T., Bookhagen, B., Blisniuk, P.M., Booth, A.L., Chamberlain, C.P., 2009. $\Delta^{18}O$ and $\delta D$ of streamwaters across the Himalaya and Tibetan Plateau: implications for moisture sources and paleoelevation reconstructions. Earth Planet. Sci. Lett. 288, 20–32. http://dx.doi.org/10.1016/j.epsl.2009.08.041.
Hutchinson, G.E., 1937. Limnological studies in Indian Tibet. Int. Rev. der gesamten Hydrobiol. und Hydrogr. 35, 134–177.
Immerzeel, W.W., van Beek, L.P.H., Bierkens, M.F.P., 2010. Climate change will affect the Asian water towers. Science 328, 1382–1385.
Jones, R.N., McMahon, T.A., Bowler, J.M., 2001. Modelling historical lake levels and recent climate change at three closed lakes, Western Victoria, Australia (c. 1840–1990). J. Hydrol. 246, 159–180.
Karim, A., Veizer, J., 2002. Water balance of the Indus River Basin and moisture source in the Karakoram and western Himalayas: implications from hydrogen and oxygen isotopes in river water. J. Geophys. Res. 107, 4362. http://dx.doi.org/10.1029/2000JD000253.
Krabbenhoft, D.P., Bowser, C.J., Anderson, M.P., Valley, J.W., 1990. Estimating groundwater exchange with lakes: 1. The stable isotope mass balance method. Water Resour. Res. 26, 2445–2453. http://dx.doi.org/10.1029/WR026i010p02445.
Leipe, C., Demske, D., Tarasov, P.E., 2014. A Holocene pollen record from the northwestern Himalayan lake Tso Moriri: Implications for palaeoclimatic and archaeological research. Quat. Int. 348, 93–112. http://dx.doi.org/10.1016/j.quaint.2013.05.005.
Lesher, R., 2011. Climate change impacts to a high altitude lake in the Indian Himalaya. Geography. San Diego State University, San Diego.
Matsuda, Y., Fujita, K., Ageta, Y., Sakai, A., 2006. Estimation of atmospheric transmissivity of solar radiation from precipitation in the Himalaya and the Tibetan Plateau. Ann. Glaciol. 43, 344–350.
Maurya, A.S., Shah, M., Deshpande, R.D., Bhardwaj, R.M., Prasad, A., Gupta, S.K., 2011. Hydrograph separation and precipitation source identification using stable water isotopes and conductivity: River Ganga at Himalayan foothills. Hydrol. Process. 25, 1521–1530. http://dx.doi.org/10.1002/hyp.7912.
Mishra, C., Humbert-Droz, B., 1998. Avifaunal survey of Tso Moriri Lake and adjoiniing Nuro Sumdo wetland in Ladakh, Indian trans-Himalaya. Forktail 14, 67–70.
Nachiappan, R.M.P., Kumar, B., 2002. Estimate of subsurface components in the water balance of Lake Nainital (Kumaun Himalaya, India) using environmental isotopes. Hydrol. Sci. J. 47, S41–S54.
Panday, P.K., Williams, C.A., Frey, K.E., Brown, M.E., 2014. Application and evaluation of a snowmelt runoff model in the Tamor River basin, Eastern Himalaya using a Markov Chain Monte Carlo (MCMC) data assimilation approach. Hydrol. Process. 28, 5337–5353. http://dx.doi.org/10.1002/hyp.10005.
Pande, K., Padia, J.T., Ramesh, R., Sharma, K.K., 2000. Stable isotope systematics of surface water bodies in the Himalayan and Trans-Himalayan (Kashmir) region. J. Earth Syst. Sci. 109, 109–115. http://dx.doi.org/10.1007/bf02719154.
Phartiyal, B., Sharma, A., Upadhyay, R., Ram-Awatar Sinha, A.K., 2005. Quaternary geology, tectonics and distribution of palaeo- and present fluvio/glacio lacustrine deposits in Ladakh, NW Indian Himalaya—a study based on field observations. Geomorphology 65, 241–256. http://dx.doi.org/10.1016/j.geomorph.2004.09.004.
Ramesh, R., Sarin, M.M., 1992. Stable isotope study of the Ganga (Ganges) river system. J. Hydrol. 139, 49–62.
Rango, A., Martinec, J., 1995. Revisiting the degree-day method for snowmelt computations. J. Am. Water Resour. Assoc. 31, 657–669.
Rozanski, K., Araguás-Araguás, L., Gonfiantini, R., 1993. Isotopic patterns in modern global precipitation. In: P.K. Swart, K.C. Lohmann, J. Mckenzie, S. Savin (Eds.), Climate Change in Continental Isotopic Records. American Geophysical Union, Washington, DC, pp. 1–37. http://onlinelibrary.wiley.com/doi/10.1029/GM078p0001/summary.
Schlup, M., Carter, A., Cosca, M., Steck, A., 2003. Exhumation history of eastern Ladakh revealed by $^{40}Ar/^{39}Ar$ and fission-track ages: the Indus River-Tso Morari transect, NW Himalaya. J. Geol. Soc. London. 160, 385–399.
Stewart, M.K., 1975. Stable isotope fractionation due to evaporation and isotopic exchange of falling waterdrops: applications to atmospheric processes and evaporation of lakes. J. Geophys. Res. 80, 1133–1146.
Tian, L., 2003. Oxygen-18 concentrations in recent precipitation and ice cores on the Tibetan Plateau. J. Geophys. Res. 108, 4293. http://dx.doi.org/10.1029/2002JD002173.
Tian, L., Yao, T., MacClune, K., White, J.W.C., Schilla, A., Vaughn, B., Vachon, R., Ichiyanagi, K., 2007. Stable isotopic variations in west China: a consideration of moisture sources. J. Geophys. Res. 112, D10112. http://dx.doi.org/10.1029/2006JD007718.
Weyhenmeyer, C.E., Burns, S.J., Waber, H.N., Macumber, P.G., Matter, A., 2002. Isotope study of moisture sources, recharge areas, and groundwater flow paths within the eastern Batinah coastal plain, Sultanate of Oman. Water Resour. Res. 38, 1184. http://dx.doi.org/10.1029/2000WR000149.
Xu, C.Y., Singh, V.P., 2000. Evaluation and generalization of radiation-based methods for calculating evaporation. Hydrol. Process. 14, 339–349.
Zhang, B., Wu, Y., Zhu, L., Wang, J., Li, J., Chen, D., 2011. Estimation and trend detection of water storage at Nam Co Lake, central Tibetan Plateau. J. Hydrol. 405, 161–170.
Zhou, S., Kang, S., Chen, F., Joswiak, D.R., 2013. Water balance observations reveal significant subsurface water seepage from Lake Nam Co, south-central Tibetan Plateau. J. Hydrol. 491, 89–99. http://dx.doi.org/10.1016/j.jhydrol.2013.03.030.
Zuber, A., 1983. On the environmental isotope method for determining the water balance components of some lakes. J. Hydrol. 61, 409–427.